A study of the structures of some (FeRu)B metallic glasses by x-ray and neutron scattering

1999 J. Phys.: Condens. Matter 11 9139

(http://iopscience.iop.org/0953-8984/11/47/302)

J. Phys.: Condens. Matter **11** (1999) 9139–9150. Printed in the UK PII: S0953-8984(99)06776-4

A study of the structures of some (FeRu)B metallic glasses by x-ray and neutron scattering

S Al-Heniti†, N Cowlam† and A R Wildes‡

† Department of Physics and Astronomy, University of Sheffield, Sheffield S3 7RH, UK
‡ Institute Laue Langevin, BP 156, 38042 Grenoble Cédex 9, France

Received 9 August 1999

Abstract. The atomic scale structures of the ruthenium substituted metallic glasses $Fe_{83-x}Ru_xB_{17}$ and $Fe_{80-x}Ru_xB_{20}$ have been studied by x-ray and neutron scattering. The addition of up to 22% of ruthenium causes an ≈5% increase in the first neighbour distance, while the co-ordination number stays roughly constant around the value $n_1 \approx 12.5 \pm 0.5$. The evolution in the shape of the first peak in the radial distribution function is consistent with the new atomic correlations introduced by the addition of ruthenium. The higher real space resolution in the neutron experiments allows the first neighbour transition metal–boron correlations to be identified. The substitution of the larger transition metal causes little change in the structural order in these glasses, which are confirmed to be suitable candidates for the study of collinear and non-collinear magnetic structures in ferromagnetic metallic glasses. The variation of the magnetization of these glasses with composition can be described in an empirical way or in the context of percolation theory. Neither model requires the presence of non-collinear moments. According to the latter description the magnetization M appears to have a power law dependence on composition $M = (x - x_c)^\beta$. The magnitude of $\beta = 0.39$ is close to the expected value, although the critical concentration $x_c = 0.595$ is much greater than the values predicted by percolation theory.

1. Introduction

The transition metal–metalloid (TM–met) metallic glasses which contain iron, cobalt or nickel and one or more of the metalloids (B, Si, P) normally have compositions close to a eutectic (e.g. $Fe_{83}B_{17}$). They generally exhibit soft ferromagnetic properties and are the subject of considerable scientific interest and of applications in a variety of devices, including transformers, sensors, magnetic tags and recorder heads.

The glass forming ranges of these alloys are broadened by the addition of a second transition metal or a second metalloid to the parent eutectic alloy. The magnetic properties of these quasi-binary TM–met glasses have been extensively studied, in the search for the optimized samples for technological applications. The variations of the average magnetic moment and the Curie temperature with composition follow the same trends as in binary crystalline TM alloys (see figure 2 of [1]). The rapid reduction in magnetic moment when a second transition metal is substituted into $Fe_{80}met_{20}$ or $Co_{80}met_{20}$, for example, has been attributed to simple dilution effects or alternatively to an antiferromagnetic alignment of a large (free atom size) magnetic moment on the substituted atoms. The very soft magnetic properties of these glasses were originally attributed to genuine collinear ferromagnetic structures, but more recently evidence has emerged from a range of different measurements (see [2], [3] and

0953-8984/99/479139+12$30.00

references therein) to suggest that non-collinear arrangements of the magnetic moments are present.

Neutron scattering measurements with polarization of the incident and scattered beams in which four spin dependent scattering cross sections are measured [4] provide the most direct way of searching for non-collinear magnetic structures [2, 5, 6]. In one standard configuration [4] the neutron polarization (and also the magnetic field applied to the sample) are perpendicular to the scattering plane. In this case, the neutron *spin-flip* cross sections (see [2, 4, 6]) contain information on *transverse* components of the magnetic moments within the scattering plane and the *non-spin-flip* cross sections contain information about the *collinear* components along the field direction. The equations describing the scattering cross sections in terms of the spin components S_x, S_y, S_z are given in [4, 6]. We have established unequivocal evidence for the presence of non-collinear magnetic structures in the archetypal $Fe_{83}B_{17}$ glass using this technique [5]. We have also shown that $(Fe_xNi_{1-x})_{78}B_{12}Si_{10}$ glasses exhibit complex magnetic structures in which the nickel atoms carry magnetic moments comparable to those on the iron atoms, but which are randomly orientated and do not contribute to the net moment when a magnetic field is applied [2].

Going beyond the first row of the transition metals, $Fe_{80-x}Ru_xB_{20}$ metallic glasses with compositions $0 \leqslant x \leqslant 22$ exhibit interesting changes in magnetic behaviour [7, 8]. They are ferromagnetic for $x = 0$ to $x \approx 16$ and for $16 \leqslant x \leqslant 19$ they are re-entrant spin glasses. Alloys with $x = 20$ to 22 transform on cooling from the paramagnetic state directly into a phase with spin-glass-like behaviour. Thus the rapid decline of magnetic moment with the addition of ruthenium and the disorder in the directions of the magnetic moments in the spin glass phases [7, 8] suggested that these would be good candidates in the search for non-collinear ferromagnetic structures. We recently made polarized beam neutron measurements on a series of three samples of $Fe_{80-x}Ru_xB_{20}$ metallic glasses with $x = 0$, 10 and 18% [6]. The presence of the non-collinear structures in $Fe_{80}B_{20}$ was confirmed, but surprisingly non-collinear structures were absent from the two ruthenium substituted samples.

The presence of non-collinear magnetic structures in metallic glasses has stimulated considerable theoretical interest and the development of sophisticated electron band theory calculations (e.g. [9]). The predictions of these calculations are so detailed that there may be few experimental methods which can test them effectively. These theoretical advances make it imperative that the structures and homogeneity of the ferromagnetic metallic glasses are tested most rigorously, so that the non-collinear ferromagnetism is shown to be an intrinsic property and not a result of some unforeseen defects in the samples. This has been the purpose of the present study. A series of seven $Fe_{83-x}Ru_xB_{17}$ metallic glass samples has been studied by x-ray scattering and a further three $Fe_{80-x}Ru_xB_{20}$ samples by x-ray and neutron scattering methods. The visibility of the boron is improved by a factor of about nine in the neutron experiments. In addition, the iron atoms scatter more strongly than ruthenium by a factor of 1.7:1, in contrast to the x-ray case, where the ratio is 2.9:1 in the opposite sense. The time-of-flight neutron experiments also provide substantially improved resolution in real space.

2. Sample preparation, experimental method and data analysis

Three large samples of $Fe_{80-x}Ru_xB_{20}$ metallic glasses with composition $x = 0$, 10 and 18% were prepared for polarized beam neutron scattering experiments on the IN20 instrument at the Institute Laue Langevin. A second series of seven $Fe_{83-x}Ru_xB_{17}$ samples with compositions $x = 0$, 5, 10, 15, 18, 20 and 22% was prepared for a detailed investigation of their glassy structures, as these had not been examined in the studies of their magnetic properties made elsewhere [7, 8].

Spectrographically pure iron rod (99.98%), ruthenium sponge (99.9%) and boron crystalline pieces (99.7%) were supplied by Aldrich Chemicals Ltd. Isotopically enriched boron was not used as it may cause problems with the viscosity of the melt, possibly by contaminants. Appropriate quantities of the elements were melted and thoroughly mixed in an argon arc furnace. The resulting master ingot of 20 g was divided into four pieces which were each melt-spun in helium atmosphere onto a steel wheel. The metallic glass ribbon produced was ≈1 mm wide and ≈25 μm thick. X-ray samples were made by winding this ribbon onto the usual aluminium holder to obtain a flat surface in reflection geometry, with the ribbon direction along the incident beam. The x-ray measurements were performed using a Philips PW1050 vertical diffractometer with molybdenum Kα radiation $\lambda = 0.711$ Å and a curved crystal monochromator. A standard scan of 18 h was used which covered scattering angles $5^\circ < 2\theta < 160^\circ$ in two stages and an equivalent background run was made. The total structure factors $S(Q)$ were derived from the absolute scattered intensities, using an average value of the normalization constants from different established methods [10].

The $S(Q)$ curves for the three $Fe_{80-x}Ru_xB_{20}$ samples and for the seven $Fe_{83-x}Ru_xB_{17}$ samples are shown at the top and bottom of figure 1 respectively. The forms of these total $S(Q)$ curves confirm that the ten different (FeRu)B samples are genuine metallic glasses. They exhibit all the classic features of the $S(Q)$ of metallic glasses, namely a sharp first peak, which here lies in the range $3.03 < Q_1 < 3.11$ Å^{-1}; a second peak with the characteristic shoulder on its large Q side and further oscillations about unity to $Q \approx 14$ Å^{-1}. The full width at half maximum (FWHM) of the first peak is $\Delta Q \approx 0.56$ Å^{-1} for all the samples, which corresponds to a 'range of structural variations' $r_s \approx 2\pi/\Delta Q \approx 11$ Å. Table 1 gives some parameters from the $S(Q)$ curves shown in figure 1. They show that the width of the first peak remains sensibly constant and the change of its position with composition is consistent with the introduction of the larger ruthenium atoms. In fact, all the $S(Q)$ curves superimpose quite well, which suggests that any systematic differences in their form are probably lost in statistical noise of the data points.

The similarity between the $S(Q)$ can be explained by considering the (FeRu)B glasses as pseudo-binary ⟨TM⟩–B, where ⟨TM⟩ means the average of the transition metals iron and ruthenium. $S(Q)$ can then be expressed in terms of the partial structure factors

$$S(Q) = \omega_{\langle TM\rangle\langle TM\rangle} S_{\langle TM\rangle\langle TM\rangle}(Q) + \omega_{\langle TM\rangle B} S_{\langle TM\rangle B}(Q) + \omega_{BB} S_{BB}(Q) \qquad (1)$$

where the ω_{ij} weighting factors [15] are given by

$$\omega_{\langle TM\rangle\langle TM\rangle} = \frac{x^2\phi^2_{\langle TM\rangle}}{\langle\phi\rangle^2} \qquad \omega_{\langle TM\rangle B} = \frac{2x(1-x)\phi_{\langle TM\rangle}\phi_B}{\langle\phi\rangle^2} \qquad \omega_{BB} = \frac{(1-x)^2\phi_B^2}{\langle\phi\rangle^2}.$$

ϕ is the scattering amplitude whose average value is $\langle\phi\rangle = x\phi_{\langle TM\rangle} + (1-x)\phi_B$ with x, $(1-x)$ the atomic concentrations. Evaluating equation (1) with ϕ equal to the atomic scattering factor $f(Q)$ gives for the parent $Fe_{83}B_{17}$

$$S(Q) = 0.926S_{FeFe}(Q) + 0.073S_{FeB}(Q) + 0.001S_{BB}(Q)$$

and for the glass with the most ruthenium $Fe_{61}Ru_{22}B_{17}$

$$S(Q) = 0.937S_{\langle TM\rangle\langle TM\rangle}(Q) + 0.062S_{\langle TM\rangle B}(Q) + 0.001S_{BB}(Q).$$

These equations are valid in the limit $Q = 0$. They show that the ω_{ij} change by only ≈1%, so that the $S(Q)$) are expected to be similar across the composition range studied.

Planar samples for neutron diffraction were wound on flat frames with brass sides and steel wire stretchers (30 mm × 25 mm) originally designed for the IN20 experiments. The measurements were performed in transmission geometry on the Liquid and Amorphous

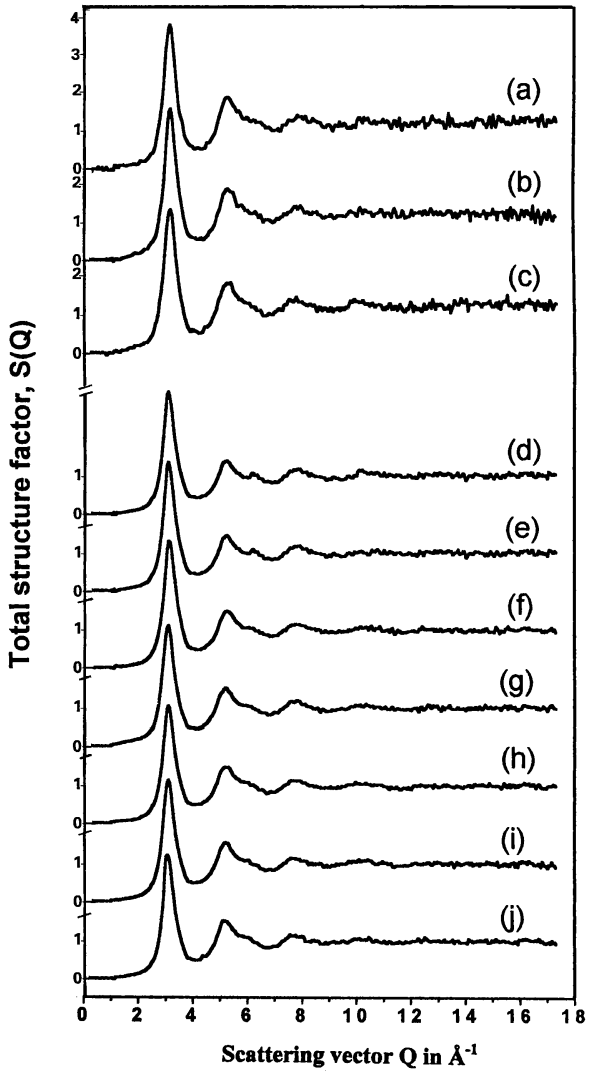

Figure 1. The total structure factors $S(Q)$ of the three $Fe_{80-x}Ru_xB_{20}$ metallic glasses (a)–(c) and of the seven $Fe_{83-x}Ru_xB_{17}$ metallic glasses (d)–(j) obtained by x-ray diffraction are given. The identification of the compositions (a)–(j) is the same as in tables 1 and 2.

Diffractometer (LAD) at the ISIS facility at Rutherford Appleton Laboratory [11]. The samples were supported on a brass frame with suitable cadmium shields and the ribbon direction was vertical. Scan times of approximately 3 h per sample were used and a vanadium calibration and a background scan were also made. The raw time-of-flight data were reduced and corrected for sample and instrumental factors using the ATLAS suite of programs [12]. The total $S(Q)$ for each sample was obtained by merging the data from the different detectors, excluding those at 5 and 90°, for reasons of difficult Placzek corrections and sample shielding respectively. The $I(0)$, $I(\infty)$, normalization method was used. The resulting curves for the three glasses are shown in figure 2 and their parameters are given in table 2. They exhibit the same characteristic features as the curves in figure 1 described above. They are of excellent statistical quality

Table 1. The positions of the first, second and second peak shoulder in the total structure factors of the (FeRu)B metallic glasses are given together with the width of the first peak. The identification of the compositions (a)–(m) is the same as in figures 1–4.

Glass composition	Position of peaks in $S(Q)$ (Å^{-1}) ($\pm$0.05)			
	Q_1	Q_2	Q_{2S}	ΔQ
With x-rays				
$Fe_{80}B_{20}$ (a)	3.14	5.30	6.21	0.56
$Fe_{70}Ru_{10}B_{20}$ (b)	3.16	5.27	6.21	0.57
$Fe_{62}Ru_{18}B_{20}$ (c)	3.12	5.25	5.92	0.59
$Fe_{83}B_{17}$ (d)	3.11	5.26	6.23	0.55
$Fe_{78}Ru_5B_{17}$ (e)	3.09	5.23	6.23	0.56
$Fe_{73}Ru_{10}B_{17}$ (f)	3.11	5.31	6.06	0.56
$Fe_{68}Ru_{15}B_{17}$ (g)	3.03	5.20	5.94	0.57
$Fe_{65}Ru_{18}B_{17}$ (h)	3.09	5.25	6.06	0.56
$Fe_{63}Ru_{20}B_{17}$ (i)	3.07	5.23	5.94	0.55
$Fe_{61}Ru_{22}B_{17}$ (j)	3.07	5.26	5.94	0.55
With neutrons				
$Fe_{80}B_{20}$ (k)	3.14	5.28	6.08	0.55
$Fe_{70}Ru_{10}B_{20}$ (l)	3.13	5.21	6.01	0.55
$Fe_{62}Ru_{18}B_{20}$ (m)	3.09	5.22	6.02	0.55

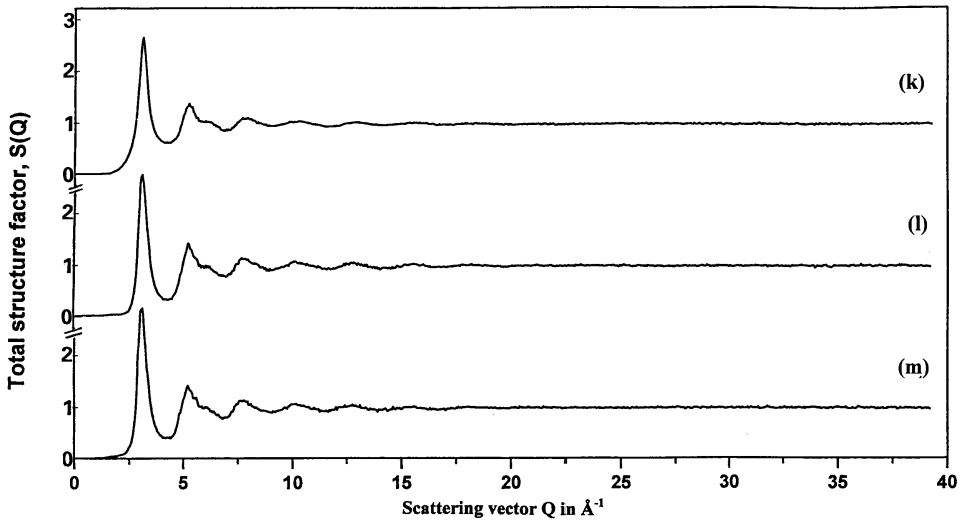

Figure 2. The total structure factors $S(Q)$ of the three $Fe_{80-x}Ru_xB_{20}$ metallic glasses (k)–(m) obtained by neutron diffraction are given. Eight oscillations in $S(Q)$ can be seen by viewing the figure obliquely. The identification of the three compositions is the same as in tables 1 and 2.

(recalling that each neutron scan took just 3 h), so that the eighth oscillation in $S(Q)$ at $Q \approx 21$ Å^{-1} is just visible with careful scrutiny. The accuracy of the level $S(Q) \equiv 1$ beyond $Q \approx 25$ Å^{-1} is a tribute to the correctness of the data analysis. Some systematic differences can be seen between these better defined curves. The base of the first peak is broadest for the parent $Fe_{80}B_{20}$ glass, although the FWHM is the same for the three samples, $\Delta Q \approx 0.55$ Å^{-1}.

Table 2. The positions of the peaks and their ratios in the reduced RDFs $G(r)$ of the (FeRu)B metallic glasses are given, together with the co-ordination number n_1 obtained from the RDF. The values of n_1 in brackets refer to the transition metal–boron first neighbour correlations. The identification of the compositions (a)–(m) is the same as in figures 1–4.

Glass composition	Peak positions from $G(r)$ (Å) (±0.05) and peak ratios (±0.02)					n_1 (±0.02) from RDF
	r_1'	r_1	r_2/r_1	r_{2S}/r_1	$\langle r_1^G \rangle$	
With x-rays						
$Fe_{80}B_{20}$ (a)		2.54	1.68	1.95	2.50	12.2
$Fe_{70}Ru_{10}B_{20}$ (b)		2.57	1.64	1.91	2.52	12.1
$Fe_{62}Ru_{18}B_{20}$ (c)		2.58	1.72	1.95	2.54	11.9
$Fe_{83}B_{17}$ (d)		2.51	1.69	1.93	2.51	12.5
$Fe_{78}Ru_5B_{17}$ (e)		2.56	1.70	1.90	2.52	12.5
$Fe_{73}Ru_{10}B_{17}$ (f)		2.58	1.69	—	2.53	12.4
$Fe_{68}Ru_{15}B_{17}$ (g)		2.59	1.70	1.91	2.54	12.2
$Fe_{65}Ru_{18}B_{17}$ (h)		2.60	1.70	—	2.54	12.2
$Fe_{63}Ru_{20}B_{17}$ (i)		2.61	1.69	—	2.55	12.3
$Fe_{61}Ru_{22}B_{17}$ (j)		2.62	1.67	—	2.55	12.5
With neutrons						
$Fe_{80}B_{20}$ (k)	2.14	2.57	1.64	1.91	2.44	(1.6) 11.3
$Fe_{70}Ru_{10}B_{20}$ (l)	2.14	2.57	1.63	1.95	2.46	(1.8) 11.9
$Fe_{62}Ru_{18}B_{20}$ (m)	2.15	2.58	1.67	1.94	2.47	(1.9) 11.5

3. The structures of (FeRu)B metallic glasses

The reduced RDF $G(r)$ for each glass was obtained from the Fourier transform of the x-ray $S(Q)$ shown in figure 1

$$G(r) = 4\pi r[\rho(r) - \rho_0] = \frac{2}{\pi}\int_0^{Q_{max}} Q[S(Q) - 1]M(Q)\sin(Qr)\,\mathrm{d}Q$$

which was evaluated with the modification function $M(Q)$ proposed by Lorch [13]. These $G(r)$ curves, which are all very similar in form [14], will not be presented here. The positions of the first peak are in the range $2.50 < r_1 < 2.63$ Å, see table 2, so the addition of 22% of ruthenium to the $Fe_{83}B_{17}$ glass produces only a ≈5% increase in the first neighbour distance. The ratios of the positions of the first peak to the second and to its shoulder fall within the usually accepted ranges 1.67–1.70 and 1.90–1.93. The neighbour distances r_n are best obtained from the reduced RDF $G(r)$ because it lacks the parabolic background of the RDF from which the co-ordination number n_1 is obtained.

$$\mathrm{RDF}(r) = 4\pi r^2\rho(r) = rG(r) + 4\pi r^2\rho_0.$$

The RDFs derived from the x-ray data on the seven $Fe_{83-x}Ru_xB_{17}$ glasses are shown in figure 3. The values of n_1 which were obtained by integrating the area of the first peak up to the minimum at $r \approx 3.2$ Å are given in table 2 and they do not change significantly from $n_1 \approx 12.5 \pm 0.5$ over the composition range studied. However a detailed examination of figure 3 shows there are slight changes to the *shape* of the first peak in the RDF with composition which are attributable to the new neighbour distances to the ruthenium atoms. The RDF may be written as the sum of partial pair correlation functions $\rho_{ij}(r)$

$$\mathrm{RDF}(r) = 4\pi r^2\sum_{i,j}\omega_{ij}\rho_{ij}(r)$$

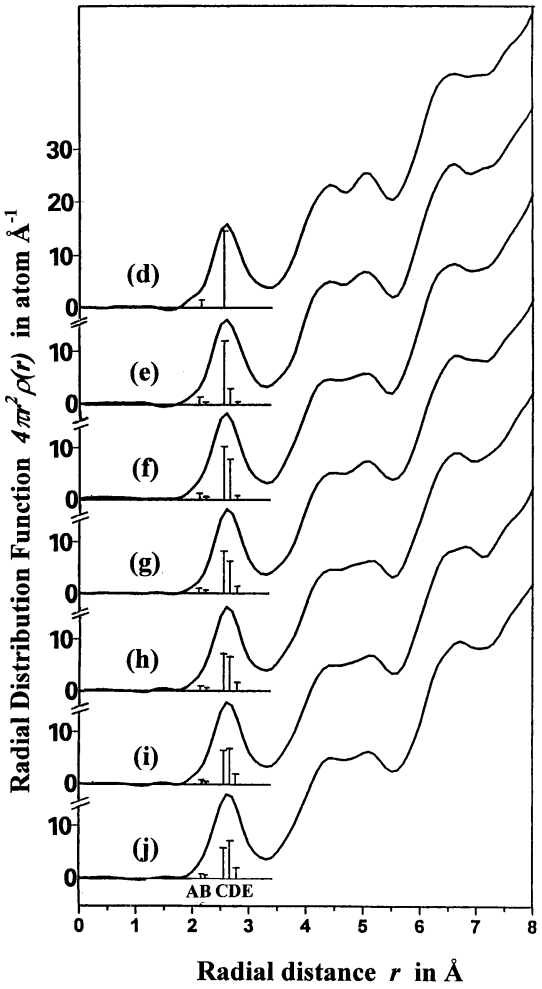

Figure 3. The RDFs of the seven $Fe_{83-x}Ru_xB_{17}$ metallic glasses (identified (d)–(j) obtained by x-ray diffraction are given. The vertical bars are designed to give a visual indication of the following pair correlations: A = Fe–B; B = Ru–B; C = Fe–Fe; D = Fe–Ru and E = Ru–Ru in the first peak. (The x-ray equivalent data for the three $Fe_{80-x}Ru_xB_{20}$ samples have been presented elsewhere [14] to avoid repetition.)

with the same weighting functions ω_{ij} defined above. Thus for $Fe_{83}B_{17}$, the RDF may be written, in ascending order of first neighbour distances,

$$\mathrm{RDF}(r) = 4\pi r^2(0.001\rho_{BB}(r) + 0.073\rho_{FeB}(r) + 0.926\rho_{FeFe}(r)).$$

If the (FeRu)B glasses are considered as true ternary alloys, they have six partial pair correlations so that the RDF for $Fe_{78}Ru_5B_{17}$ becomes

$$\mathrm{RDF}(r) = 4\pi r^2(0.001\rho_{BB}(r) + 0.063\rho_{FeB}(r) + 0.007\rho_{RuB}(r) + 0.765\rho_{FeFe}(r) + 0.164\rho_{FeRu}(r) + 0.009\rho_{RuRu}(r)).$$

Figure 4 shows how the changing shape of the first peak in RDFs can be interpreted in terms of these summations. The vertical bars represent the following first neighbour pair correlations: A = Fe–B; B = Ru–B; C = Fe–Fe; D = Fe–Ru and E = Ru–Ru and are designed to give

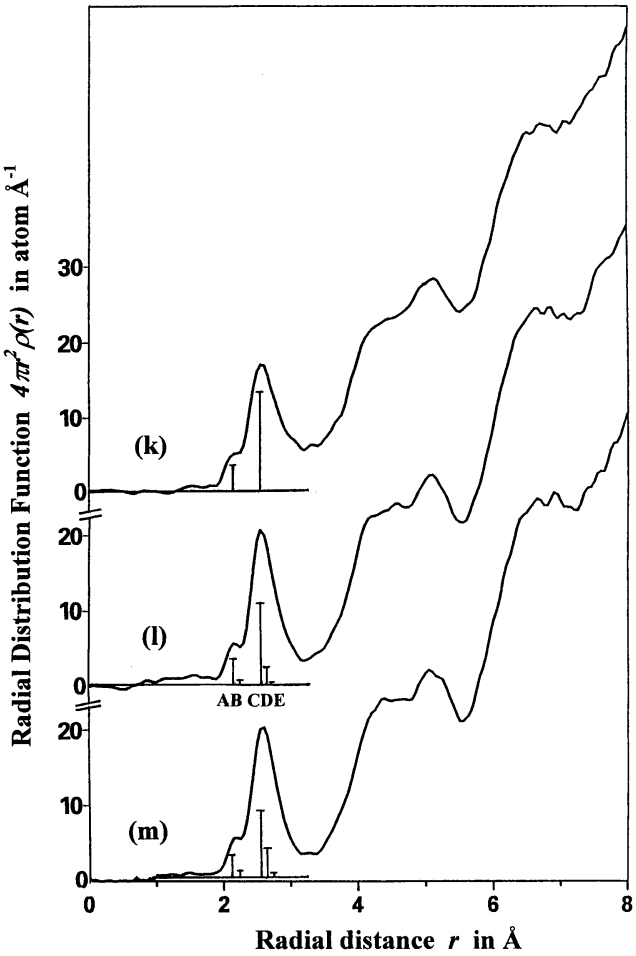

Figure 4. The RDFs of the three $Fe_{80-x}Ru_xB_{20}$ metallic glasses (identified (k)–(m) obtained by neutron diffraction are given. The vertical bars A–E represent the same partial pair correlations as in figure 3.

a visual indication of the contribution of each to the first peak. Their radial positions are derived from the Goldschmidt radii for the metals $r^G_{Fe} = 1.27$ Å, $r^G_{Ru} = 1.34$ Å and the tetrahedral covalent radius of boron $r^T_B = 0.88$ Å, to give $r_{FeB} = 2.15$ Å; $r_{RuB} = 2.22$ Å; $r_{FeFe} = 2.54$ Å; $r_{FeRu} = 2.61$ Å and $r_{RuRu} = 2.68$ Å. For the glass $Fe_{61}Ru_{22}B_{17}$ at the limit of the composition range studied here, table 3 shows that the Fe–Ru correlations have the highest weighting. Together with the Ru–Ru correlations they account for approximately 60% of the first neighbour peak and they shift it to higher radial distances. The weighting factors ω_{ij} can also be used to calculate the effective first neighbour distance from the pair distances given above. Here the weighting factors are important since both the *presence* and the *visibility* of each pair correlation must be taken into account. These calculated values $\langle r^G_1 \rangle$ are given in table 2 and they are all just slightly smaller than the values of r_1 derived from the experimental $G(r)$. Finally, note that drawing the heights of the vertical bars in proportion to the weighting factors ω_{ij} strictly implies that the occupation of the first neighbour shell is random. It would be necessary to evaluate the partial pair correlation functions to

Table 3. Examples of the weighting factors ω_{ij} for the partial structure factors (and for the partial pair correlation functions) are given for the parent, binary FeB glasses and for selected ternary (FeRu)B glasses. They are presented in ascending order of first neighbour distances.

Glass composition	Weighting factors ω_{ij}					
	ω_{BB}	ω_{FeB}	ω_{RuB}	ω_{FeFe}	ω_{FeRu}	ω_{RuRu}
With x-rays						
$Fe_{83}B_{17}$ (d)	0.001	0.073	—	0.926	—	—
$Fe_{78}Ru_5B_{17}$ (e)	0.001	0.063	0.007	0.765	0.164	0.009
$Fe_{61}Ru_{22}B_{17}$ (j)	0.001	0.039	0.024	0.361	0.441	0.135
With neutrons						
$Fe_{80}B_{20}$ (k)	0.015	0.216	—	0.769	—	—
$Fe_{70}Ru_{10}B_{20}$ (l)	0.016	0.199	0.022	0.622	0.134	0.007
$Fe_{62}Ru_{18}B_{20}$ (m)	0.017	0.185	0.040	0.510	0.224	0.025

establish whether there were any special correlations between the iron and the ruthenium atoms.

A similar analysis has also been made of the RDFs of the three $Fe_{80-x}Ru_xB_{20}$ obtained from the neutron data shown in figure 4, where the ω_{ij} weighting factors have been evaluated with $\phi = b$, the nuclear scattering length. Table 3 shows that for the two parent binary glasses, the weighting factor ω_{FeB} is about three times larger with neutrons than with x-rays. Also the visibility of the ruthenium atoms is much reduced with neutrons so that the combined value of ω_{FeB} and ω_{RuB} for the $Fe_{62}Ru_{18}B_{20}$ glass are commensurate with ω_{FeRu}. The improved real space resolution is important in determining the shape of the first peak in figure 4. The theoretical resolution in these diffraction experiments is $\Delta r = 2\pi/Q_{max}$ but the real figure will be slightly larger because of the Lorch modification function used for both x-ray and neutron data. The effective Q_{max} will relate to the point in $S(Q)$ beyond which there is little information content in the function. Thus taking values $Q_{max} \approx 12$ Å^{-1} and $Q_{max} \approx 25$ Å^{-1} gives $\Delta r \approx 0.52$ Å and $\Delta r \approx 0.25$ Å for the x-ray and neutron data respectively.

A separate sub-peak can therefore be seen on the low r side of the first peak in the RDFs of figure 4 for all three samples, which can be identified with the Fe–B and Ru–B first neighbour correlations from the first neighbour distances given above. A partial co-ordination number can be obtained on the assumption that this peak is symmetrical about its maximum, and this yields the values $n_{\langle TM\rangle B} = 1.6$–$1.9$ given in brackets in table 2. These $n_{\langle TM\rangle B}$ are in reasonable agreement with similar values obtained elsewhere [16, 17]. The total co-ordination number obtained by integrating the whole of the first peak up to a distance of $r = 3.2$ Å has values $n_1 = 11.3$–11.9. These are slightly smaller than the values obtained with x-rays and this is probably due to the better definition of the first minimum in the RDF. Note that it is not feasible to determine partial co-ordination number for the transition metal atoms from the *difference* between n_1 and $n_{\langle TM\rangle B}$, because the remainder of the first peak cannot be uniquely identified with ⟨TM⟩ correlations [2]. An unusual feature of the three RDFs shown in figure 4 is that the first minimum is not well developed for the parent $Fe_{80}B_{20}$. It is likely that the broadening at the base of the first peak of the $S(Q)$ for the $Fe_{80}B_{20}$ glass, referred to above, is responsible for this. Certainly the amplitudes of the first peak and the first minimum of the two ruthenium substituted glasses are in better accord with the amplitudes observed by Sváb *et al* [16] in similar high resolution neutron measurements on $Fe_{81}B_{19}$ metallic glass. However the lack of spurious ripple in the $G(r)$ of the $Fe_{80}B_{20}$ glass [14], and the fact that its co-ordination number is similar to the other two compositions, suggest that the derivation of its $S(Q)$ must be substantially correct.

4. Structural and magnetic properties of (FeRu)B metallic glasses

The $S(Q)$ and RDF curves presented here contain all the classic and established features which show that the (FeRu)B samples are good metallic glasses. The x-ray and neutron measurements demonstrate that addition of up to 22% ruthenium to the eutectic alloy $Fe_{83}B_{17}$ alloy, and up to 18% ruthenium to the $Fe_{80}B_{20}$ composition, does not cause any *abrupt* structural changes in the two series of glasses studied.

On the other hand, the value of the net magnetic moment derived from magnetization measurements falls slowly at first and then more rapidly with the addition of ruthenium to $Fe_{80}B_{20}$ glass [8] and this is also mirrored in the variation of Curie temperature with composition [7]. The net magnetic moment per transition metal $\mu_{\langle TM\rangle}$ obtained from [8] is shown in the top part of figure 5. This variation cannot be described by a simple dilution with $\mu_{Ru} = 0$ alone,

$$\mu_{\langle TM\rangle} = \frac{(80-x)\mu_{Fe} + x\mu_{Ru}}{80} \Rightarrow \left(1 - \frac{x}{80}\right)\mu_{Fe}$$

which is shown by the dashed line in the figure. However, if the magnetic moment on the iron falls according to the fraction (e.g. [18]) of first neighbour iron atoms,

$$\mu_{Fe}^{eff} \propto \frac{(80-x)\mu_{Fe}^{80}}{80}$$

then the inclusion of this extra term describes the initial slow decrease of $\mu_{\langle TM\rangle}$,

$$\mu_{\langle TM\rangle} = \left(1 - \frac{x}{80}\right)^2 \mu_{Fe}$$

as shown by the dash–dot line in figure 5. However it would be necessary to make an additional assumption that an (increasing) fraction $(1-K)$ of these magnetic moments are antiferromagnetically aligned with respect to the majority (K), to describe the precipitous fall in $\mu_{\langle TM\rangle}$ beyond 15% ruthenium so that

$$\mu_{\langle TM\rangle} = \left(1 - \frac{x}{80}\right)^2 (2K-1)\mu_{Fe}.$$

The values of K can be found from the 'expected' and actual values of $\mu_{\langle TM\rangle}$. The fraction of these antiferromagnetically aligned magnetic moments is zero for glasses with less than 15% ruthenium and then $(1-K)$ increases monotonically from 0.12 for the $Fe_{62}Ru_{18}B_{20}$ glass to 0.38 for the $Fe_{58}Ru_{22}B_{20}$ sample [14] and this is depicted by the solid line in the figure. Note that the presence of these antiferromagnetically aligned moments cannot stimulate the presence of a non-collinear state, as this is excluded on the basis of the polarized beam neutron measurements [6]. The values of $(1-K)$ obtained do not appear to depend on the fraction of iron first neighbours. Naturally, by this third stage of the model, there must be a number of equivalent combinations of similar parameters which would produce the same degree of fit so the model cannot be taken as definitive.

An alternative to this increasingly arbitrary description is to consider that the ternary (FeRu)B glasses are based on a notional amorphous iron a-Fe_{100}, whose atomic sites are diluted by the addition of the non-magnetic elements ruthenium and boron. The (FeRu)B glasses can then be considered in terms of site percolation, in which ferromagnetism will appear at a critical concentration x_c of the iron atoms and the magnetization M will increase with composition according to a power law, $M = (x - x_c)^{\beta}$ [19]. In this case it is best to consider the average magnetic moment per atom (or site) $\langle\mu\rangle$ which is directly related to the saturation magnetization $M = N\langle\mu\rangle$. Thus, neglecting the data point for the $Fe_{58}Ru_{22}B_{20}$ sample which is in the spin glass regime, the data were replotted as shown in the lower part of figure 5 and fitted on a trial and error basis. This gave the curve $\langle\mu\rangle = 3.00(x - x_c)^{0.39}$ shown

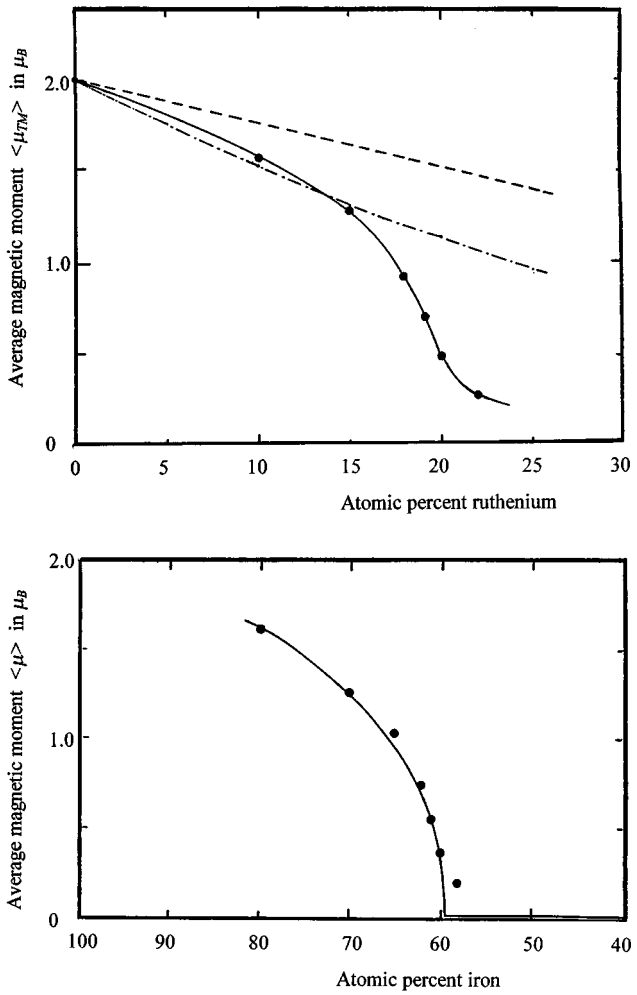

Figure 5. The variation of magnetic moment with composition for $Fe_{80-x}Ru_xB_{20}$ metallic glasses is given (after [8]). The top figure shows the reduction of the average magnetic moment on the transition metal atoms $\langle \mu_{TM} \rangle$ with the addition of ruthenium and the lines indicate the predictions of the models discussed in the text. The bottom figure depicts the onset of ferromagnetism and the variation of average magnetic moment per atom $\langle \mu \rangle$ described by percolation theory.

as a solid line in the figure. The value of $\beta = 0.39$ is very close to the expected one (0.41) for a three dimensional structure [19] although the critical concentration $x_c = 0.595$ is much greater than expected for either a close packed crystalline structure $x_c \approx 0.195$ [19] or an amorphous array $x_c \approx 0.27$ [20]. It has been suggested [8] that other ternary metallic glass systems which have similarly large values of x_c, such as (FeMn)–met glasses with $x_c \approx 0.65$ [21] and $(Fe_xCo_{100-x})B_y$ glasses with $x_c \approx 0.60$ [22] may have ferromagnetic and antiferromagnetic interactions. However the curve in the lower part of figure 5 gives a very satisfactory fit to the data points based on a simple dilution of a ferromagnetic species with no prior assumptions as to the moment values and no necessity to invoke the presence of non collinear magnetic structures. The curve fortuitously extrapolates to $\langle \mu \rangle = 2.11\ \mu_B$ in the limit $x = 1.0$, which is within 4% of the magnetic moment of metallic iron.

5. Conclusions

The conclusions of this study are that the (FeRu)B samples are well behaved metallic glasses whose $S(Q)$ and RDF curves exhibit all the established features. The numerical data presented in tables 1 and 2 show that the glass structures vary in a regular manner with composition. The ferromagnetic phase appears at a high ruthenium concentration and the values of magnetic moment follow a concentration dependence predicted by percolation theory. Despite the presence of disorder in the directions of the magnetic moments which is intrinsic in the spin glass and re-entrant spin glass phases, our neutron experiments with polarized beams have found no evidence of non-collinear magnetic structures in the $Fe_{70}Ru_{10}B_{20}$ and $Fe_{62}Ru_{18}B_{20}$ samples studied [6]. It will clearly be of interest now to investigate a new series of samples with low concentrations of ruthenium, to establish how rapidly the non-collinear magnetic structure in the parent binary glasses is suppressed. It will also be worthwhile to study glasses with higher ruthenium concentrations using neutron small angle scattering, to look for magnetic correlations on longer length scales than those accessible in the experiments performed to date.

Acknowledgments

The authors acknowledge the help of Mr J C Newell in the preparation of the metallic glass samples and of Dr W S Howells in the neutron diffraction experiments on LAD at ISIS. The neutron measurements were performed as part of the EPSRC neutron beam programme. NC would like to thank Dr A C Hannon for the invitation to make a contribution on 'Metallic glasses' at the LAD Celebration Meeting in March 1999. SA-H acknowledges the receipt of a grant from King Abdulaziz University, Saudi Arabia to study for a PhD.

References

[1] Mizoguchi T 1978 *Sci. Rep. RITU Suppl.* A 117
[2] Cowley R A, Patterson C, Cowlam N, Ivison P K, Martinez J and Cusson L D 1991 *J. Phys.: Condens. Matter* **3** 9521
[3] Cowlam N 1996 *J. Non-Cryst. Solids* **205–207** 567
[4] Moon R M, Riste T and Koehler W C 1969 *Phys. Rev.* **181** 920
[5] Cowley R A, Cowlam N and Cusson L D 1988 *J. Physique Coll.* C8 **49** 1285
[6] Wildes A R, Cowley R A, Al-Heniti S, Cowlam N, Kulda J and Lelièvre-Berna E 1998 *J. Phys.: Condens. Matter* **10** 2617
[7] Paulose P L, Nagarajan R, Nagarajan V and Vijayaraghavan R 1986 *J. Magn. and Magn. Mater.* **54–57** 257
[8] Paulose P L, Nagarajan R, Nagarajan V and Vijayaraghavan R 1987 *Sol. State Commun.* **61** 151
[9] Lorentz R and Hafner J 1995 *J. Magn. Magn. Mater.* **139** 207
[10] Wagner C N J 1967 *Tech. Rep. National Science Foundation* GP3213
[11] Howells W S 1980 *Rutherford Appleton Lab Report* RL-80-017
[12] Soper A K, Howells W S and Hannon A C 1989 *Rutherford Appleton Lab Report* RL-89-046
[13] Lorch E A 1969 *J. Phys. C: Solid State Phys.* **2** 229
[14] Al-Heniti S 1999 *PhD Thesis* University of Sheffield
[15] Faber T E and Ziman J M 1965 *Phil. Mag.* **13** 153
[16] Sváb E, Forgács F, Kroó N, Ishmaev S N, Sadikov I P and Chernyshov A A 1982 *Solid State Commun.* **44** 1151
[17] Nold E, Lamparter P, Olbrich H, Rainer-Harbach G and Steeb S 1981 *Z. Naturf.* a **36** 1032
[18] Vincze I, Boudreaux D S and Tegze M 1979 *Phys. Rev.* B **19** 4896
[19] Stichcombe R 1983 *Phase Transitions* vol 7 (London: Academic)
[20] Zallen R 1983 *The Physics of Amorphous Solids* (New York: Wiley)
[21] Geohegan J A and Bhagat S M 1981 *J. Magn. Magn. Mater.* **25** 17
[22] Boliang Yu, Coey J M, Olivier M and Ström-Olsen J O 1984 *J. Appl. Phys.* **55** 1748